Semiconductor Waveguide Source of Counterpropagating Twin Photons

L. Lanco,[1] S. Ducci,[1] J.-P. Likforman,[1] X. Marcadet,[2] J. A. W. van Houwelingen,[3] H. Zbinden,[3] G. Leo,[1,*] and V. Berger[1]

[1]*Laboratoire Matériaux et Phénomènes Quantiques, UMR 7162, Université Paris 7-Denis Diderot, Case 7021, 2 Place Jussieu, 75251 Paris, France*

[2]*Alcatel-Thales III-V Laboratoire, Route Départementale 128, 91767 Palaiseau Cedex, France*

[3]*Université de Genève, GAP-Optique, Rue de l'Ecole de Médecine 20, 1211 Genève 4, Switzerland*

(Received 10 July 2006; published 23 October 2006)

We experimentally demonstrate an integrated semiconductor source of counterpropagating twin photons in the telecom range. A pump beam impinging on top of an AlGaAs waveguide generates parametrically two counterpropagating, orthogonally polarized signal/idler guided modes. A 2 mm long waveguide emits at room temperature one average photon pair per pump pulse, with a spectral linewidth of 0.15 nm. The twin character of the emitted photons is ascertained through a time-correlation measurement. This work opens a route towards new guided-wave semiconductor quantum devices.

DOI: 10.1103/PhysRevLett.97.173901 PACS numbers: 42.70.Qs, 03.67.−a, 42.65.Lm, 42.65.Wi

Momentum conservation is a general property that appears in various physical contexts such as classical dynamics, optics, x-ray diffraction, and elementary particle collisions. In the field of nonlinear optics, which is the framework of the semiconductor source of twin photons described in the following, momentum conservation results in the phase matching between nonlinearly radiating dipoles. In parametric fluorescence, where one pump (p) photon is annihilated into two signal (s) and idler (i) photons sharing its energy, the translational invariance of the crystal can match the photon momentum before and after the down-conversion: $\mathbf{k_p} = \mathbf{k_s} + \mathbf{k_i}$. This is indeed the most widely used process to produce entangled photon pairs, which are one of the most intriguing phenomena at the heart of quantum mechanics [1]. Entangled two-photon states have been used to demonstrate the violation of Bell inequalities and confirm the foundations of quantum mechanics [2–4]. They are now the building block of quantum information [5], including quantum-key distribution protocols, quantum computing [6,7], or teleportation [8].

Different approaches have been followed to produce entangled two-photon states: atomic radiative cascades [2] and parametric fluorescence in nonlinear dielectric birefringent materials [3,4,9]. Compared to them, semiconductor materials fulfil stability, robustness, and integration criteria, thus exhibiting a huge potential in terms of integration of novel optoelectronic devices. A semiconductor source of entangled photons based on the biexciton cascade of a quantum dot has recently been demonstrated [10]. With respect to this technique, parametric generation in semiconductor waveguides allows room-temperature operation and a high directionality of the emission, which dramatically enhances the collection efficiency and decreases the rate of broken pairs (where one of the two photons is not collected). Moreover, the high nonlinear susceptibility of AlGaAs along with its well-mastered growth technique makes it particularly attractive for this purpose [11]. Recently, counterpropagating phase matching has attracted some interest for its potential in twin photon experiments for quantum communication [12–14], but no experimental demonstration of the generation of counterpropagating twin photons has been reported to date.

In this Letter, we use parametric fluorescence to produce counterpropagating twin photons in an AlGaAs multilayer waveguide. In our geometry, a pump beam impinging on top of a waveguide generates parametrically two counterpropagating, orthogonally polarized signal/idler guided modes through a type II interaction [Fig. 1(a)]. Counterpropagation results from the translational invariance of the waveguide along the propagation direction (z), where the momentum difference between the generated photons of a pair equals the longitudinal component of the pump momentum, $k_s - k_i = k_p \sin\theta$ [Fig. 1(b)]. In order to improve the efficiency of the nonlinear process, we implement quasiphase matching in the epitaxial direction (x) through an alternation of AlGaAs layers with different Al content and therefore different nonlinear coefficients d_{14} [15]. Important advantages result from such a geometry, in the aim of realizing quantum communication devices: absence of the pump beam in the guided direction, automatic separation of the down-converted photons and their possible coupling into two optical fibers (through standard pigtailing process), tunability through the angle of incidence of the pump beam, and the proximity of the generated photons to the Fourier transform limit [16]. Moreover, the narrow spectral bandwidth, a signature of counterpropagating processes, is beneficial in two respects: it allows long-distance propagation in optical fibers with a negligible chromatic dispersion, and most importantly for quantum optics experiments, it is well suited for the interaction with very thin transition linewidths encountered in atoms or ions.

Our sample is grown by molecular beam epitaxy on a GaAs (100) substrate; its planar structure consists of $Al_{0.94}Ga_{0.06}As$ cladding (1080 nm)/$Al_{0.25}Ga_{0.75}As$ (110 nm)/$4 \times [Al_{0.80}Ga_{0.20}As$ (124 nm)/$Al_{0.25}Ga_{0.75}As$ (110 nm)$]$/$Al_{0.94}Ga_{0.06}As$ cladding

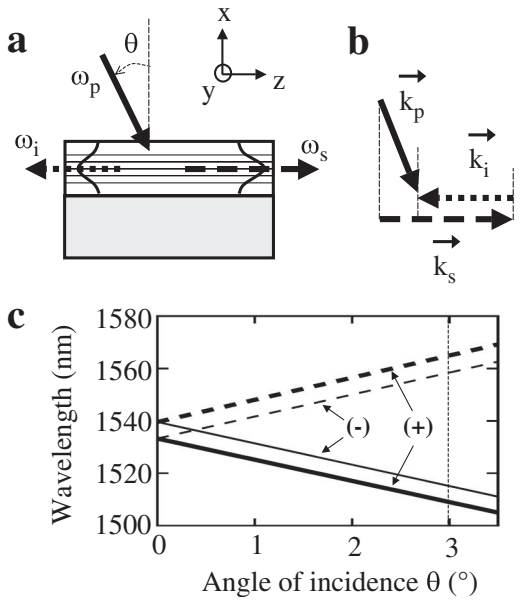

FIG. 1. Parametric generation of counterpropagating twin photons in a multilayer waveguide. (a) A pump photon of frequency ω_p is converted in two counterpropagating twin photons with frequencies ω_s and ω_i, with $\omega_s + \omega_i = \omega_p$ (energy conservation). (b) Momentum conservation is fulfilled in the longitudinal direction (z) for appropriate values of $\mathbf{k_s}$ and $\mathbf{k_i}$. (c) Calculated tuning curves for a pump wavelength 768.2 nm. Thick lines: additive interaction (+). Thin lines: subtractive interaction (−). The solid lines represent the photons copropagating with the z component of the pump beam, while the dashed lines represent the counterpropagating ones. The intersections with the vertical bar at $\theta = 3°$ are associated with the spectral measurements shown in Fig. 3.

(1080 nm). The lateral confinement is provided by a wet-etched ridge with 4 μm width and 2 mm length. AlGaAs is the material of choice to generate twin photons around 1.55 μm, compatibly to telecom devices; however, alternative materials can be used to realize a source for the silicon absorption band, for line-of-sight experiments in quantum-key distribution [17]. It is important to stress that two phase-matched processes occur simultaneously in our scheme: in the first one, the photon copropagating with the z component of the pump beam is TM polarized and the counterpropagating one is TE polarized. In the second one, the vice versa occurs.

These two processes exhibit different output spectra due to the form birefringence induced by the multilayer geometry. The sharing of the pump photon energy between signal and idler results in two concomitant effects: (1) a higher energy for the TM photon, because it travels faster than the TE photon due to birefringence; (2) a higher energy for the photon copropagating with the z projection of the pump beam, since it carries a supplementary momentum given by the pump. Additive contributions from these effects are thus obtained if the copropagating photon is TM polarized and the counterpropagating one TE polarized: this case shall hereafter be referred to as "additive" interaction. Conversely, the process with a TE copropagating photon and a TM counterpropagating photon will hereafter be referred to as "subtractive" interaction. The calculated tuning curves as a function of the pump incident angle θ are shown in Fig. 1(c): the additive interaction is responsible for the longest and shortest emitted wavelengths, whereas the subtractive interaction is responsible for the intermediate ones. We point out that the two effects discussed above (birefringence and pumping geometry) can cancel out exactly, giving rise to wavelength-degenerate twin photons. As can be seen in Fig. 1(c), this occurs for $\theta = 0.4°$ in the subtractive interaction.

From an experimental point of view, the acquisition of the time-correlation spectra of the generated photon pairs is a crucial issue. In the related setup (Fig. 2) the pump beam is provided by a TE polarized, pulsed Ti:sapphire laser with $\lambda_P = 768.2$ nm and a 3 kHz repetition rate. The pulse peak power is $P_p = 100$ W and its duration is 100 ns. The pump beam is focused on top of the waveguide ridge using a cylindrical lens (focal length = 2 cm) with an angle θ in the xz plane. The generated photons are collected with two 63× microscope objectives, spectrally analyzed with two monochromators, and then coupled into fibered InGaAs single-photon avalanche photodiodes. A time-interval analyzer records the delay $(t_s - t_i)$ between the arrival times of the generated photons.

The same experimental setup lends itself to the measurement of the spectral profiles of the generated photons,

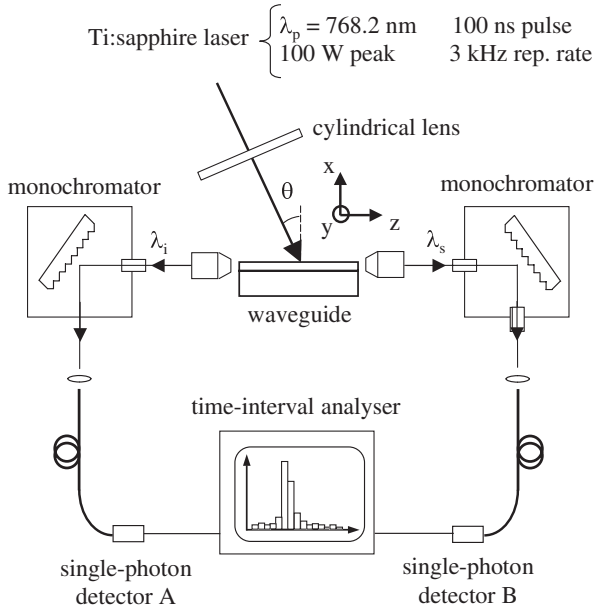

FIG. 2. Experimental setup for spectral analysis and time-correlation measurements. The generated photons are collected by two microscope objectives, sent through two monochromators, and detected by single-photon avalanche photodiodes. A time-interval analyzer records temporal correlations between the corresponding current pulses.

which are given by the count rate recorded by each detector versus wavelength. These are shown in Fig. 3 for $\theta = 3°$, where sharp peaks are superposed to a flat background. The spectral structure nicely corresponds to the expected counterpropagating processes: the longest and shortest wavelengths result from the additive process, while the intermediate ones result from the subtractive interaction. Small secondary peaks are also observed, corresponding to counterpropagating photons reflected at the waveguide facets. A complete agreement is found between experimental values and numerical simulations of the generated wavelengths. For the additive interaction, for example, the measured wavelengths deduced from Fig. 3 are 1509.5 ± 0.5 nm and 1564.5 ± 0.5 nm, where the uncertainties stem from the resolution of the monochromators. The corresponding calculated values are 1508.9 ± 1 nm and 1564.8 ± 1 nm [Fig. 1(c)]. Here the uncertainties are mainly due to the uncertainty on two inputs of our simulations: the experimental values of the incident angle ($\pm 0.05°$) and of the pump wavelength (± 0.2 nm). Such a good agreement reflects the robustness of the structure with respect to the tolerances on the ridge size (width and height) and to the fluctuations (thickness and composition of the layers) in the epitaxial process [18]. Apart from the above experimental uncertainties, the intrinsic full width at half maximum of the generated spectrum has been accurately measured by difference frequency generation and was found to be equal to 0.15 nm.

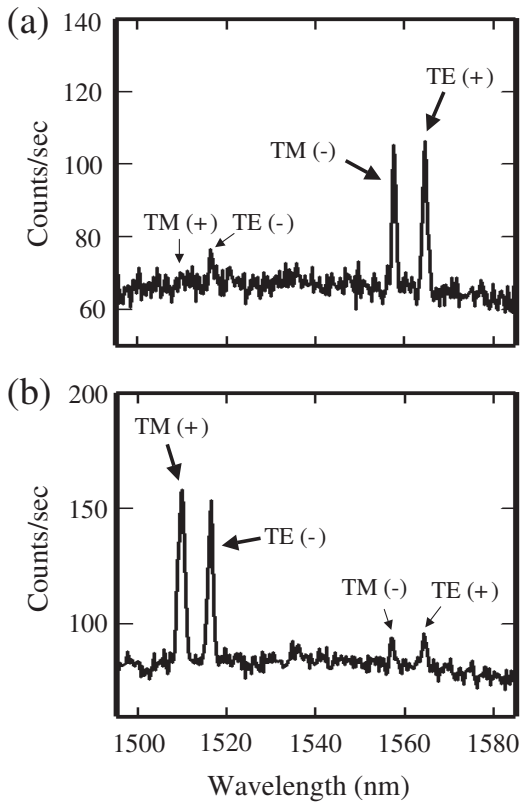

FIG. 3. Emission spectra for an angle of incidence of 3°. Spectrum (a) is acquired by the detector A of Fig. 2, and spectrum (b) is acquired by the detector B of Fig. 2. Photons copropagating with the z component of the pump (i.e., impinging on the detector B) carry a supplementary momentum, and therefore have a lower wavelength. In both spectra TM photons have a lower wavelength than the TE ones, corresponding to their higher propagation velocity in the multilayer waveguide. The small secondary peaks result from generated photons that undergo a reflection at a waveguide facet before impinging on the detector A or B.

The flat background in the measured spectra arises from two contributions: (1) dark counts generated by the detectors in the absence of any incident photon, and (2) photoluminescence due to electron-hole recombination after pump absorption, resulting from below-band-gap deep levels embedded in semi-insulating GaAs substrates. In the future, both these contributions could be reduced: the former by employing state-of-the-art detectors and the latter by partially removing the substrate.

To further assess the twin character of the emitted photons, the time correlations between the detected counts have been analyzed. A histogram of the time delays is shown in Fig. 4, for the case of the additive interaction with $\theta = 3°$. With a sampling interval of 43 ps, the histogram results from an acquisition time of 12 h. The emission level remained constant during this long integration time, which shows the remarkable robustness and stability of the device.

The peak observed for $t_s = t_i$ demonstrates unambiguously the twin character of the generated photons; the 750 ps full width at half maximum of the histogram

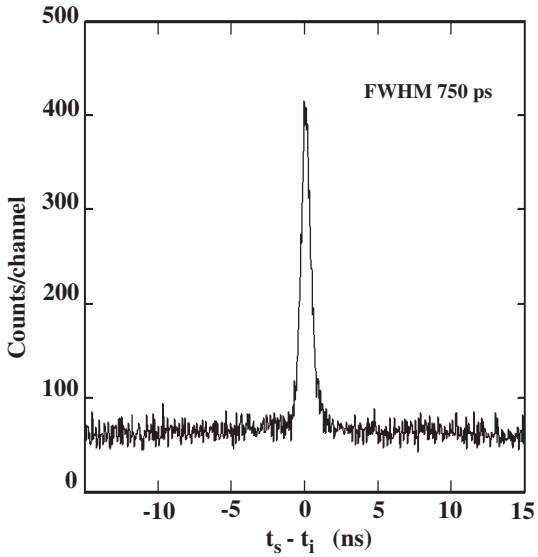

FIG. 4. Time-correlation histogram between counterpropagating photons. The peak at $t_s = t_i$ corresponds to twin photons, simultaneously generated in the additive parametric down-conversion process. The flat background corresponds to coincidences between uncorrelated counts.

corresponds to the timing jitter of both detectors. The flat background is produced by the uncorrelated coincidences with dark and below-band-gap luminescence counts: indeed, switching the pump polarization from TE to TM leads to the suppression of the $t_s = t_i$ peak, without modifying this background. Finally, no time correlation is found between photons that are generated with different interactions: this agrees with the expectations, since these photons are not generated within the same nonlinear process.

The amount of detected coincidences, 0.15 pairs per second, allows deducing the brightness of our twin photon source. Taking into account the quantum efficiency of the detectors (5%), the transmission of the monochromators (50%), and the overall transmission along the setup optical path (40%), we estimate 1500 generated pairs per second. A similar level is obtained if the subtractive interaction is selected. Finally, this leads to an average generation rate of one pair per pump pulse (or 2.5×10^{-14} generated pairs/pump photon), in good agreement with our numerical modeling. We emphasize that the above amount of average generated pairs per pulse is well suited for current standards in quantum-key distribution protocols.

Moreover, significant improvements in quantum efficiency and background noise suppression are expected with a structure including Bragg mirrors to enhance the light-matter interaction and by removing the GaAs substrate, source of spurious deep level emission events. These modifications (especially the microcavity immersion) will lower the pump power to standard pump sources below the Watt level. Before these improvements, the source reported in this Letter generates more pairs (one per pump pulse) than necessary for quantum information. Compared to the guided twin photon sources reported to date in periodically poled lithium niobate waveguides [19] and in photonic crystal fibers [20], our source exhibits room-temperature operation, very narrow bandwidth, no need for pump spectral cleaning (the pump is not guided), and easy separation of the generated photons. Finally, we emphasize the possibility of directly generating polarization-entangled states. For example, the generation of a Bell state can be done by simultaneously pumping the sample with $\theta = \pm 0.4°$ [see Fig. 1(c)], by illuminating the waveguide through a diffraction grating [13] or by inserting it in a bow-tie cavity.

Clearly, our twin photon source can be profitably integrated in innovative devices. On the one hand, one can, e.g., obtain an entangled light emitting diode thanks to the integration of an electrically pumped vertical cavity surface-emitting laser on top of the waveguide. On the other hand, forgetting entanglement but making use of simultaneity, an integrated heralded source of single photons is readily available by integrating or pigtailing a photon counter at one of the two waveguide facets.

These innovations can be envisaged because our source belongs to the domain of semiconductors, which is a major qualitative leap of our work. Because of all these advantages and perspectives, we candidate our twin-photon-source geometry as a novel archetype for future quantum information devices.

The authors would like to thank Pascal Filloux for ridge processing and Marco Ravaro for experimental help. This work has been funded by IST Project No. 2001-38864 RAMBOQ of the European Union.

*Corresponding author.
Electronic address: leo.giuseppe@paris7.jussieu.fr

[1] D. Bouwmeester, D. Eckert, and A. Zeilinger, *The Physics of Quantum Information* (Springer, New York, 2000).
[2] A. Aspect, P. Grangier, and G. Roger, Phys. Rev. Lett. **49**, 91 (1982).
[3] W. Tittel, J. Brendel, H. Zbinden, and N. Gisin, Phys. Rev. Lett. **81**, 3563 (1998).
[4] G. Weihs, T. Jennewein, C. Simon, H. Weinfurter, and A. Zeilinger, Phys. Rev. Lett. **81**, 5039 (1998).
[5] T. Jennewein, C. Simon, G. Weihs, H. Weinfurter, and A. Zeilinger, Phys. Rev. Lett. **84**, 4729 (2000).
[6] D. Deutsch and E. Ekert, Phys. World **11**, 47 (1998).
[7] P. Walther, K. J. Resch, T. Rudolf, E. Schenck, H. Weinfurter, V. Vedral, M. Aspelmeyer, and A. Zeilinger, Nature (London) **434**, 169 (2005).
[8] D. Bouwmeester, J. W. Pan, K. Mattle, M. Eibl, H. Weinfurter, and A. Zeilinger, Nature (London) **390**, 575 (1997).
[9] P. G. Kwiat, K. Mattle, H. Weinfurter, A. Zeilinger, A. V. Sergienko, and Y. H. Shih, Phys. Rev. Lett. **75**, 4337 (1995).
[10] R. M. Stevenson, R. J. Young, P. Atkinson, K. Cooper, D. A. Ritchie, and A. J. Shields, Nature (London) **439**, 179 (2006).
[11] A. Fiore, V. Berger, E. Rosencher, P. Bravetti, and J. Nagle, Nature (London) **391**, 463 (1998).
[12] Y. J. Ding, S. J. Lee, and J. B. Khurgin, Phys. Rev. Lett. **75**, 429 (1995).
[13] A. De Rossi and V. Berger, Phys. Rev. Lett. **88**, 043901 (2002).
[14] M. C. Booth, M. Atature, G. Di Giuseppe, B. E. A. Saleh, A. Sergienko, and M. C. Teich, Phys. Rev. A **66**, 023815 (2002).
[15] M. Ravaro, Y. Seurin, S. Ducci, G. Leo, V. Berger, A. De Rossi, and G. Assanto, J. Appl. Phys. **98**, 063103 (2005).
[16] E. Knill, R. Laflamme, and G. J. Milburn, Nature (London) **409**, 46 (2001).
[17] S. Ducci, V. Berger, A. De Rossi, G. Leo, and G. Assanto, J. Opt. Soc. Am. B **22**, 2331 (2005).
[18] L. Lanco, S. Ducci, J.-P. Likforman, M. Ravaro, P. Filloux, X. Marcadet, G. Leo, and V. Berger, Appl. Phys. Lett. **89**, 031106 (2006).
[19] S. Tanzilli, H. de Riedmatten, W. Tittel, H. Zbinden, P. Baldi, M. de Micheli, D. B. Ostrowski, and N. Gisin, Electron. Lett. **37**, 26 (2001).
[20] J. G. Rarity, J. Fulconis, J. Duligall, W. J. Wadsworth, and P. St. J. Russell, Opt. Express **13**, 534 (2005).